

# Electronic structure of zinc-blende $\text{Al}_x\text{Ga}_{1-x}\text{N}$ ; Screened-Exchange Study

Byounggak Lee\* and Lin-Wang Wang

*Computational Research Division, Lawrence Berkeley National Laboratory, Berkeley, California 94720*

We present a first principle investigation of the electronic structure and the band gap bowing parameter of zinc-blende  $\text{Al}_x\text{Ga}_{1-x}\text{N}$  using both local density approximation and screened-exchange density functional method. The calculated sX-LDA band gaps for GaN and AlN are 95% and 90% of the experimentally observed values, respectively, while LDA underestimates the gaps to 62% and 70%. In contrast to the gap itself, the band gap bowing parameter is found to be very similar in sX-LDA and LDA. Because of the difference in the conduction band structure, the direct to indirect band gap crossover is predicted to occur at different Al concentration.

PACS numbers: 71.15.Mb, 71.20.-b, 71.23.-k, 71.55.Eq

The group-III nitrides have long been studied for photoelectronic applications, such as ultraviolet<sup>1</sup>/blue<sup>2</sup>/green<sup>3</sup> light-emitting diodes and lasers. The control of emitted light in wide range frequency is possible by harnessing the large band gap differences of parent compounds through alloy fabrication. Therefore, understanding the band gap behavior of disordered alloys is valuable for designing materials with desirable properties. There have been many theoretical works for the band gap dependence on the alloy concentrations for various semiconductor alloys. Most of such previous studies were carried out using local density approximation (LDA) of the density functional theory. While LDA is reliable in calculating the atomic relaxation and formation energies of the semiconductor alloys, the calculation of their band gaps is hindered by its intrinsic errors in describing the excited states. There is no clear understanding of whether the LDA band gap errors in pure bulk crystals will cause significant errors in the band gap behavior in the alloy, especially for quantities such as the bowing parameters.

While the LDA method has severely underestimated the band gap of pure III-nitrides,<sup>4,5</sup> the screened-exchange density functional method (sX-LDA) has been successful in many III-V semiconductors.<sup>6,7</sup> Implemented using a Thomas-Fermi screening scheme, sX-LDA improves the LDA band gap similar to that of many-body GW calculations and also yields the ground state structure as good as LDA. Although the sX-LDA method has been systematically studied for simple II-V, III-V, IV-IV semiconductor compounds, the calculations for more complicated systems like vacancy, surface and alloys are relatively scarce. This is partly because the sX-LDA calculation, while computationally cheaper than the GW method, is still much more expensive than the LDA calculation. In the current work we test the applicability of sX-LDA for semiconductor alloy systems by comparing its results with experimental measurements and available GW calculations. We choose the  $\text{Al}_x\text{Ga}_{1-x}\text{N}$  alloy due to the intense recent interest on these systems for potential wide gap device applications. We study  $\text{Al}_x\text{Ga}_{1-x}\text{N}$  alloys in zinc-blende structure, and focus on the band gap

bowing and the crossover of direct and indirect band gap.

The calculations were carried out using a plane-wave basis with Troullier-Martins norm-conserving pseudopotentials.<sup>8</sup> We performed the LDA calculations both with Ga 3*d* electrons in the valence and with Ga 3*d* electrons in the core but representing their effects with a nonlinear core correction. We found that, for bulk GaN, including the Ga 3*d* electrons in the valence reduces the band gap by  $\sim 0.3$  eV. For the sX-LDA calculations, including 3*d* electrons in the valence causes a significant error in the pseudopotential calculations. This is because the exchange integrals between the 3*d* wavefunctions and the 3*p*, 3*s* wavefunctions are distorted by the use of the pseudo-wavefunctions instead of the original all electron wavefunctions. These effects and the corresponding ways to correct them will be addressed in a separate paper. In the current study, we did not include the 3*d* electrons in the valence in the sX-LDA calculation. As long as both calculations are done with Ga 3*d* electrons in the core, the comparison between sX-LDA and LDA is valid. When compared with experimental measurements, the  $\sim 0.3$  eV correction from the GaN side can be added to sX-LDA results in a posterior process. For III-nitrides, the valence band maximum state is strongly localized near N atoms and, as a result, the valence band spin-orbit splitting is small; e.g., 11 meV for GaN and even smaller for AlN.<sup>9</sup> Subsequently, the spin-orbit coupling was not included in our calculations.

In Fig. 1, we show the electronic structure of zinc-blende GaN and AlN calculated from LDA and sX-LDA both without the Ga 3*d* states. In these bulk calculations, the integration over the Brillouin zone was done by sampling 19 special *k*-points in an irreducible wedge. The kinetic energy cutoff in all calculations (including the alloys) is 70 Ryd. The direct band gap at  $\Gamma$  point and the indirect band gap at *X* point are listed in Table I. Our band structure calculation reveals that zinc-blende GaN and AlN have band gaps at  $\Gamma$  and *X* point, respectively. While GaN and AlN crystalize in wurtzite structure under ambient conditions, GaN has been found in zinc-blende structure when epitaxially grown<sup>10,11</sup>, thus we have calculated zinc-blende structure for the alloys. In order to compare with experimental band gaps which

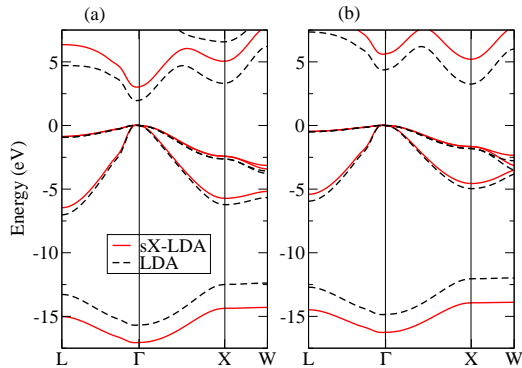


FIG. 1: The electronic band structure of zinc-blende nitrides, (a) GaN and (b) AlN. The solid lines are the sX-LDA results and the dashed lines are the LDA results. The bands are adjusted so that VBM energy is located at zero. Experimental lattice constant  $a = 4.5 \text{ \AA}$  for GaN and  $a = 4.3 \text{ \AA}$  for AlN were used.

are in wurtzite structure, we need to relate zinc-blende band gaps to wurtzite band gaps. According to previous studies,<sup>12</sup> the wurtzite  $\Gamma$  point band gap is close to the zinc-blende  $\Gamma$  point band gap and that the possible indirect band gap of wurtzite is at  $U$  point, which is located at two-thirds of the  $M$ - $L$  distance away from  $M$  point, with a value similar to the average of the zinc-blende  $L$  point energy is rather high for AlN, the wurtzite AlN crystal has a direct band gap,<sup>13</sup> which should be compared with the direct band gap of zinc-blende AlN. The experimental direct band gap of wurtzite GaN scatters between 3.2-3.35 eV.<sup>14-16</sup> Our sX-LDA result, 3.04 eV, agrees well with the experiments and corresponding GW band gap.<sup>13</sup> On the other hand, LDA underestimates the gap by  $\sim 40\%$ . For AlN the experimentally measured direct band gap for wurtzite structure is 6.28 eV,<sup>9</sup> and the sX-LDA zinc-blende  $\Gamma$  point band gap of 5.63 eV is smaller than experiments and the GW band gap of 6.0 eV. Just as in GaN, the LDA calculation severely underestimates band gap of AlN. Another feature in Table I is the fact that, while sX-LDA band gap at  $\Gamma$  point is smaller than GW prediction, the  $X$  point gap is larger. The same phenomenon has been observed in other bulk materials. For example, in GaAs sX-LDA overestimates the  $X$  point energy  $\sim 0.4$  eV.<sup>6</sup> Another effect of sX-LDA on the band structures of both GaN and AlN is the increase of the valence band width by  $\sim 2$  eV, which agrees with the GW calculation.<sup>13</sup>

Besides the band gap, we also look into the self-consistent charge density changes from LDA to sX-LDA. Fig. 2 shows the radially averaged charge density centered around each constituent atoms in GaN and AlN. Electrons are highly localized on N atoms and the bond

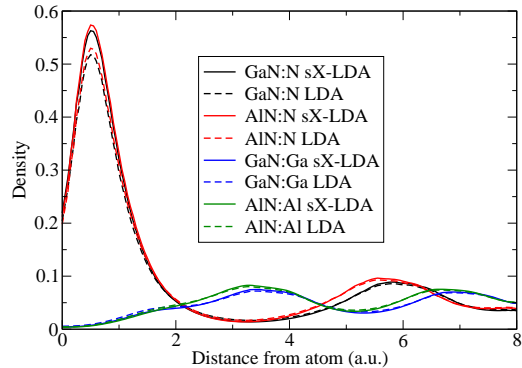


FIG. 2: Radially averaged charge density from the constituent atoms. Solid lines are from sX-LDA and dashed lines are from LDA.

charge is displaced toward N atoms from its nominal bond center position. We observe that, within the same method, the charge density around N atoms does not significantly change from GaN to AlN. Because the erroneous self-interaction in LDA is partially corrected in sX-LDA, the sX-LDA produces a larger charge transfer towards the N atoms. Similar effect has been observed in other semiconductors, such as Si and GaAs, where sX-LDA produces a stronger bond charge.

To model the disordered zinc-blende  $\text{Al}_x\text{Ga}_{1-x}\text{N}$  alloy with Al molar fraction  $0 < x < 1$ , we employed special quasi-random structures (SQSs).<sup>17</sup> SQSs are finite model systems constructed to mimic the radial correlation functions of an infinite random structure. They have been extensively used to study the electronic structures of alloys. We considered two classes of model systems of SQS8 and SQS16. In SQS8 the cell consists of  $n$  Al,  $m$  Ga, and 8 N atoms with  $n + m = 8$ . In SQS16 the cell contains twice the number of atoms in SQS8. For each model system, the lattice constant was inferred from experimental lattice constant using Vegard's law.<sup>18</sup> The equilibrium atom positions were obtained by minimizing the total energy within LDA. A total of 16  $k$ -point were used to integrate over SQS Brillouin zone for SQS8. Table II shows that, compared with SQS16, the SQS8 LDA band gaps are already converged. Thus we used SQS8 in our following calculations. Table II also shows the calculation results

TABLE I: Band gap of zinc-blende GaN and AlN in eV.

	LDA	sX-LDA	GW <sup>13</sup>
GaN $E_g(\Gamma_{15}^v \rightarrow \Gamma_1^c)$	1.97	3.04	3.1
GaN $E_g(\Gamma_{15}^v \rightarrow X_1^c)$	3.31	5.05	4.7
AlN $E_g(\Gamma_{15}^v \rightarrow \Gamma_1^c)$	4.39	5.63	6.0
AlN $E_g(\Gamma_{15}^v \rightarrow X_1^c)$	3.26	5.21	4.9

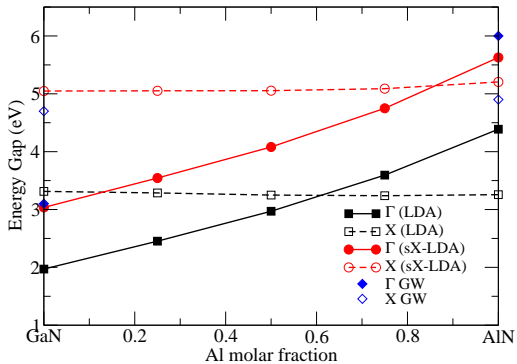


FIG. 3: Band gap dependence of  $\text{Al}_x\text{Ga}_{1-x}\text{N}$  on Al molar fraction  $x$ . The energy gap is the difference between the VBM at  $\Gamma$  point and the CBM at  $\Gamma$  point, filled symbols, or  $X$  point, empty symbols. The quasi-particle GW results are from the calculation by A. Rubio *et al.*<sup>13</sup>

including Ga 3d states in the valence. Qualitatively, they are similar to the results without including Ga 3d states in the valence.

We now study the band gap dependence of  $\text{Al}_x\text{Ga}_{1-x}\text{N}$  on Al concentration,  $x$ . We show the band energy difference between the valence band maximum (VBM) and the conduction band minimum (CBM) in Fig. 3. We trace separately the direct  $\Gamma$  point and indirect  $X$  point band gaps. For  $X$  point, since SQS unit cells have less symmetry than the pure zinc-blende crystal, we averaged the  $X$  point energies over the three  $X$  points. The bowing parameters of the direct and the indirect optical gaps are given in Table III. Both LDA and sX-LDA bowing parameters are quite small and are within the experimentally measured range of 0.6 - 1.0 eV.<sup>19-21</sup> Although the experimental discrepancy in the measured bowing parameter prevents us from making a more precise comparison, we can conclude that the calculated sX-LDA and LDA bowing parameters are similar and that they are both close to experiment. From the similarity of the sX-LDA and LDA results we infer that there are no serious consequences due to the band gap error of LDA in the bowing parameter calculations of these systems and also that sX-LDA can be reliably applied to

TABLE II: The LDA band gap dependence on SQS cell size and Ga pseudopotentials. Band gaps (eV) of  $\text{Al}_x\text{Ga}_{1-x}\text{N}$  at  $\Gamma$  point with Al molar fraction  $x$  are listed.

	0	0.25	0.5	0.75	1.0
SQS8 without Ga 3d	1.97	2.45	2.97	3.59	4.39
SQS8 with Ga 3d	1.66	2.16	2.72	3.42	4.39
SQS16 without Ga 3d	1.97	2.47	2.96	3.62	4.39

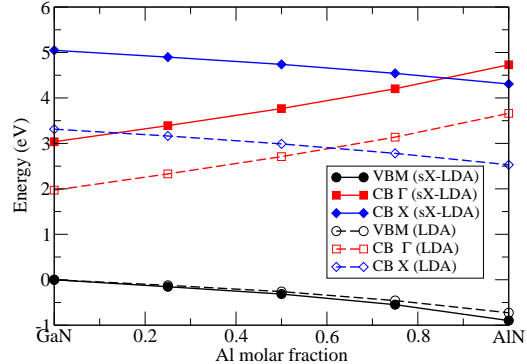


FIG. 4: Band edge states of  $\text{Al}_x\text{Ga}_{1-x}\text{N}$ . The reference energy of each method is the VBM of GaN.

this alloy system.

A distinct feature in Fig. 3 is the crosses of the direct and indirect band gaps and the change of the position of this cross introduced by sX-LDA. The LDA result shows the crossover at  $x=0.61$  while sX-LDA shows it at  $x=0.85$ . To further understand this behaviors, we show the energy levels of different states separately in Fig. 4. We have aligned the top of valence band between the LDA and sX-LDA results. Note that we have changed the lattice constant of SQS's at different Al concentration according to Vegard's law and, as a result, that the changes of energy levels reflect the effects of the lattice constant as well as the Al concentration. First we see that, after the band alignment, the change of VBM due to the use of sX-LDA is very small. For the conduction band  $\Gamma$  point energy, the difference between sX-LDA and LDA is almost a rigid shift. For the  $X$  point, the up shift at the AlN side is slightly larger than the GaN side. More importantly, the overall shift for the  $X$  point energy is larger than the  $\Gamma$  point shift. This difference causes the crossover shifts to a larger  $x$  value. Unfortunately, this larger up-shift for the  $X$  point is probably an artifact of sX-LDA, which stems from its bulk calculation. Thus this sX-LDA predicted crossover position might not be reliable. This implies that, although sX-LDA can be used for alloy calculations, in order to make more accurate quantitative predictions for complex systems, it is required to improve the bulk band structures over all

TABLE III:  $\text{Al}_x\text{Ga}_{1-x}\text{N}$  bowing parameter for the direct ( $\Gamma$ ) and indirect ( $X$ ) optical gaps in eV.

	$b_\Gamma$	$b_X$
LDA	0.83	0.13
sX-LDA	1.00	0.29

Brillouin zone, not just at the  $\Gamma$  point. This raises the necessity of exploring other forms of screening model. Only after the bulk band structures are improved, sX-LDA can be reliably applied to larger and more inhomogeneous systems such as alloys.

In summary, we tested sX-LDA for bulk GaN and AlN, and found that the calculated band gaps are closed to the experiments and other quasiparticle GW calculations. We also calculated the bowing parameter of  $\text{Al}_x\text{Ga}_{1-x}\text{N}$  and found that, in spite of the large band gap correction, the bowing parameter is similar in sX-

LDA and LDA. This confirms that both LDA and sX-LDA is equally reliable for band gap bowing parameter calculations. We also point out that it is necessary to further improve the sX-LDA formalism for its bulk band structures in order to provide quantitative predictions for other features, such as the  $\Gamma$ - $X$  crossover point.

We thank S.-H. Wei for providing with the SQSs. This work was supported by U.S. Department of Energy under contract No. DE-AC03-76SF00098 and the calculations were done using resources of NERSC at Lawrence Berkeley National Lab.

- 
- \* Electronic address: [bhlee@lbl.gov](mailto:bhlee@lbl.gov)
- <sup>1</sup> S. Nakamura, *Semicond. Sci. Technol.* **14**, R27 (1999).
  - <sup>2</sup> S. Nakamura, *The Blue Laser Diode GaN based Light Emitters and Lasers* (Springer, Berlin, 1997).
  - <sup>3</sup> S. Nakamura, M. Senoh, N. Iwasa, S. Nagahama, T. Yamada, and T. Makai, *Japan. J. Appl. Phys.* **34**, L1332 (1995).
  - <sup>4</sup> A. F. Wright and J. S. Nelson, *Phys. Rev. B* **51**, 7866 (1995).
  - <sup>5</sup> C. Stampfl and C. G. Van de Walle, *Phys. Rev. B* **59**, 5521 (1999).
  - <sup>6</sup> A. Seidl, A. Görling, P. Vogl, J. A. Majewski, and M. Levy, *Phys. Rev. B* **53**, 3764 (1996).
  - <sup>7</sup> C. B. Geller, W. Wolf, S. Picozzi, A. Continenza, R. Asahi, W. Mannstadt, A. J. Freeman, and E. Wimmer, *Appl. Phys. Lett.* **79**, 368 (2001).
  - <sup>8</sup> N. Troullier and J. Martins, *Solid State Commun.* **74**, 613 (1990).
  - <sup>9</sup> O. Madelung, M. Schulz, and H. Weiss, eds., *Intrinsic Properties of Group IV Elements and III-V, II-VI, and I-VII Compounds*, vol. 22 Pt. a of *Landolt-Bornstein, New Series* (Springer, Berlin, 1987).
  - <sup>10</sup> M. PAISLEY, Z. SITAR, J. POSTHILL, and R. DAVIS, *J. Vac. Sci. Technol.* **7**, 701 (1989).
  - <sup>11</sup> E. Martinez-Guerrero, E. Bellet-Amalric, L. Martinet, G. Feuillet, B. Daudin, H. M. H. P. Holliger, C. Dubois, C. Bru-Chevallier, P. Nze, et al., *J. Appl. Phys.* **91**, 4983 (2002).
  - <sup>12</sup> C.-Y. Yeh, S.-H. Wei, and A. Zunger, *Phys. Rev. B* **50**, R2715 (1994).
  - <sup>13</sup> A. Rubio, J. L. Corkill, M. L. Cohen, E. L. Shirley, and S. G. Louie, *Phys. Rev. B* **48**, 11810 (1993).
  - <sup>14</sup> W. R. L. Lambrecht, B. Segall, S. Strite, G. Martin, A. Agarwal, H. Morkoç, and A. Rockett, *Phys. Rev. B* **50**, 14155 (1994).
  - <sup>15</sup> A. Trampert, O. Brandt, and K. H. Ploog, in *Semiconductors and Semimetals*, edited by J. I. Pankove and T. D. Moustakas (Academic, San Diego, 1998), vol. 50.
  - <sup>16</sup> I. Vurgaftman, J. R. Meyer, and L. R. Ram-Mohan, *J. Appl. Phys.* **89**, 5815 and reference therein (2001).
  - <sup>17</sup> S.-H. Wei, L. G. Ferreira, J. E. Bernard, and A. Zunger, *Phys. Rev. B* **42**, 9622 (1990).
  - <sup>18</sup> L. Vegard, *Z. Phys.* **5**, 17 (1921).
  - <sup>19</sup> S. R. Lee, A. F. Wright, M. H. Crawford, G. A. Petersen, J. Han, and R. M. Biefeld, *Appl. Phys. Lett.* **74**, 3344 (1999).
  - <sup>20</sup> F. Yun, M. A. Reshchikov, L. He, T. King, H. Morkoç, S. W. Novak, and L. Wei, *J. Appl. Phys.* **92**, 4837 (2002).
  - <sup>21</sup> N. Nepal, J. Li, M. L. Nakarmi, J. Y. Lin, and H. X. Jiang, *Appl. Phys. Lett.* **87**, 242104 (2005).